THE FORMATION OF SURFACE Ti-Al-V-Cu ALLOY BY COMBINED ION-PLASMA TREATMENT

A.V. Basalai[1], N.N. Cherenda[2], A.B. Petukh[2], V.V. Uglov[2], A.P. Laskovnev[1], A.Yu. Isobello[1], V.M. Astashinski[3], A.M. Kuzmitski[3]

[1]Physical Technical Institute, National Academy of Sciences of Belarus, Kuprevicha str., 10, Minsk 220141, Belarus

[2]Belarusian State University, Nezavisimosti ave., 4, Minsk 220030, Belarus

[3]A.V. Luikov Heat and Mass Transfer Institute, National Academy of Sciences of Belarus, P. Brovki str., 15, Minsk 220072, Belarus

Keywords: titanium alloy Ti-6Al-4V, copper, compression plasma flow, phase and element composition, microhardness, friction coefficient

Abstract

In this work surface Ti-Cu-Al-V alloy was synthesized by compression plasma flows impact on Ti-6Al-4V titanium alloy preliminary coated by copper. The treatment of Cu/ Ti-6Al-4V samples was carried out by three pulses of compression plasma flows generated in the nitrogen atmosphere (energy density absorbed by the surface was varied in the range of 26 -43 J/cm^2 per pulse). The phase and elemental composition, structure, microhardness and friction coefficient of the formed surface alloy were investigated. It has been established that plasma treatment resulted in the formation of α-Ti solid solution containing alloying elements in the surface layer and δ-TiN on the surface. Increase of the energy absorbed by the surface during plasma impact led to decrease of Cu concentration (2.7-0.5 at.%) in the analyzed layer. The surface alloy was characterized by a uniform distribution of Ti, Al, and V atoms in contrast to the distribution of these elements on the surface of the untreated Ti-6Al-4V alloy. The microhardness increase up to 4.7 GPa (1.3 times higher in comparison with initial Ti-6Al-4V alloy) was found after compression plasma flows treatment at 43 J/cm^2. Tribological tests showed that the minimal friction

coefficient (0.13) was observed after treatment at the absorbed energy density of 26 J/cm^2.

Introduction

Titanium alloys are widely used in the manufacture of medical implants. The most common titanium-based alloy is ($\alpha + \beta$) -alloy Ti-6Al-4V due to its strength properties and high corrosion resistance (Kaur et.al., 2019; Khorosani et.al., 2015). However, in a number of works it was noted that the use of Ti-Al-V type alloy in medicine as components of endoprostheses can cause complications in the human body due to the toxicity of vanadium and aluminum (Mohammed et.al., 2014). In addition, the increase in the number of arthroplasty operations entails the increase in the number of infectious complications. Bacterial infection is one of the common causes of failure of titanium-based implants. Therefore, the development of Ti alloys with bacterial inhibiting properties is an urgent task.

Improvement of antibacterial properties can be achieved by additional surface alloying of the Ti-6Al-4V alloy with copper atoms (Li et.al., 2019). Copper has a high antimicrobial efficiency and was chosen as an element forming a new titanium-based alloy with antibacterial properties (Zhang et.al., 2013; Wang et.al., 2019). Copper is an essential element of several enzymes and a metabolizable agent, it is also capable to enhance vascularization and promote osteogenic differentiation and bone healing, and has low cytotoxicity. In addition, copper has a low cost compared to other antimicrobial materials (Ag, Au, Pd, Pt).

Synthesis of copper containing surface layer in Ti-6Al-4V alloy by the combined action of ion-plasma flows and investigation of it structure, elemental and phase composition, properties were the main aims of this work.

Experimental

The formation of a titanium-based surface alloy containing copper was carried out by preliminary deposition of a copper coating with a thickness of ~ 1 μm on samples of the Ti-6Al-4V alloy by the method of vacuum cathode-arc deposition and subsequent exposure to compression plasma flows (CPF). The samples were processed by three pulses of CPF at an initial voltage across the capacitor bank of 4 kV. The discharge duration was ~ 100 μs. Before the discharge, the pre-evacuated vacuum chamber of the MPC was filled with a working gas (nitrogen) up to a pressure of 400 Pa. The distance between the sample and the cathode cut of the electric discharge system was varied in the range of 8-14 cm. Growth of the distance causes decrease in the energy absorbed by the sample surface during plasma impact in the range of 26-43 J/cm^2. The surface morphology of the samples was studied using scanning electron microscopy (SEM) on a LEO1455VP microscope. The elemental composition of the samples was determined by X-ray spectral microanalysis (X-ray microanalysis) using Oxford X-ray detector coupled to a scanning electron microscope. The phase composition was investigated by X-ray diffraction analysis using a RIGAKU Ultima IV diffractometer in the geometry of a parallel beam in Cu Kα radiation. The microhardness of the samples under study was measured on a Wilson Instruments 402MVD device with a load on the indenter of 0.5 N. Tribological tests were carried out on a TAU-1M setup (according to the «finger – plane» scheme) with the reciprocating motion of an indenter made of VK8 hard alloy at a speed of 4 mm/s under conditions of dry friction for 30 min. The load on the indenter was 1 N.

Results and Discussion

CPF impact on the coating/substrate system led to the melting of the coating and the surface layer of the substrate, their liquid-phase mixing, and subsequent ultrafast cooling (up to 10^7 K/s) (Astashinski et.al., 2016). Thus CPF treatment of Cu/ Ti-6Al-4V samples resulted in formation of titanium-based surface alloy containing Cu, Al and V. Besides that additional doping with nitrogen atoms diffusing from residual atmosphere of a vacuum chamber took place (Cherenda et. al., 2012).

According to the X-ray microanalysis data (Table), the content of the main alloying elements (aluminum and vanadium) in the initial sample corresponded to the grade composition for the Ti-6Al-4V alloy. The incorporation of additional alloying elements (copper and nitrogen) reduced the relative concentration of aluminum and vanadium due to the normalization of concentration to 100%. The concentration of copper decreased with the growth of the energy density absorbed by surface layer, that is associated with the erosion of the surface layer under plasma exposure and increase of the molten layer thickness (Cherenda et. al., 2015, Cherenda et. al., 2019). According to the metallographic analysis of the samples cross- sections, the thickness of the molten layer was changed from 16 μm (at Q = 26 J/cm^2) to 26 μm (at Q=43 J/cm^2). Since erosion affects the elemental composition of the surface, thereby influencing its properties, the change in the mass of the samples of the system after plasma impact was investigated (Figure 1). One can see that increase of the absorbed energy density led to the growth of the mass removed from the surface. This dependence had almost linear character within the error of mass measurement. Linear dependences of the removed mass on the number of pulses and certain regions of the absorbed energy density of CPF treatment were observed for steel, beryllium bronze and copper (Cherenda et. al., 2015).

Table. Concentration of elements, wt.%

Investigated system	Energy density Q, J/cm^2	Concentration of elements, wt. %				
		Ti	Al	V	Cu	N
Ti-6Al-4V	-	89.9	6.1	4.0	-	-
Cu/Ti-6A-4V	26	84.8	4.3	3.5	2.7	4.7
	30	85.5	4.5	3.5	1.9	4.6
	37	86.7	4.5	3.4	0.9	4.5
	43	87.4	4.6	3.4	0.5	4.1

Figure 2 shows the distributions of titanium, copper, aluminium and vanadium along the surface of the initial sample Ti-6Al-4V (Fig. 2a) and the sample of the

Cu/Ti-6Al-4V system after CPF impact with an absorbed energy density of 26 J / cm^2 (Fig. 2 b). As can be seen from Fig. 2 b, the molten layer was characterized by a uniform distribution of Ti, Al, and V atoms (even at the minimum energy of the CPF impact), in contrast to the distribution of these elements on the surface of the initial sample (Fig. 2 a).

The change in the elemental composition of the surface layer led to the surface layer phase composition change (Figure 3). In the coated sample, the α-Ti diffraction lines were shifted towards larger diffraction angles relative to the α-Ti standard because the main phase of the Ti-6Al-4V alloy was α-Ti (Al, V) substitutional solid solution.

No diffraction lines of copper were observed on the diffraction patterns of the samples after CPF impact. At the same time «shoulders» appeared on the left side of all diffraction lines of α-Ti which may indicate the formation of an additional phase based on α-Ti with a larger lattice parameters, e.g. martensitic phase or solid solution with the participation of impurity atoms larger than titanium atom. The intensity of the lines of this phase decreased with an increase of the energy density absorbed by the surface. In addition, the appearance of δ-TiN lines was observed, the intensity of which increased with an increase of the absorbed energy density. Lattice parameter of δ-TiN was smaller than that of the standard indicating formation of a solid solution on the basis of titanium nitride crystalline lattice. The formation of nitride after the action of the CPF can be explained by interaction of titanium atoms on the surface with the atoms of the residual atmosphere of the vacuum chamber at the stage of the surface layer cooling after the decay of the plasma flow (Astashinski et.al., 2016).

The formation of a nitride film on the alloy surface was confirmed by the data of scanning electron microscopy (Figure 4). Surface nitride film possessed dendritic structure at all treatment regimes. Formation of such structure can be explained by crystallization in conditions of high cooling speed.

The size of dendrites depends on the value of supercooling and, consequently, on the temperature gradient in the liquid, the speed of movement of the crystallization front and the initial concentration of impurities in the melt (Astashinski et.al., 2016). Grain average size was about 2 μm in this experiment. The formation of similar dendritic structures was previously obtained during nitriding of a titanium alloy of technical purity using a CPF (Astashinski et.al., 2016).

The above-described changes in the structure, elemental and phase composition of the surface under the action of CPF on the Ti 6Al 4V alloy with a pre-deposited copper coating led to an increase in the microhardness of the surface layer (Figure 5). The microhardness of the initial sample of the Ti-6Al-4V alloy was 3.65 GPa. 1.2-1.3 times increase of the surface layer microhardness was observed for all CPF treatment regimes. Several factors could influence on surface microhardness: microstructure dispersion, δ-TiN formation and crystalline lattice distrosion due to solid solution formation on the basis of the change in the concentration of elements in solid solutions of α-Ti.

The results of tribological tests showed that in the initial sample, the average value of the coefficient of friction in the steady-state friction mode was 0.25 after passing 4 m (Figure 6). After CPF impact the friction coefficient decreased for all treatment regimes: 0.15 at Q= 43 J/cm^2 and 0.13at Q=26 J/cm^2. As it can be seen from the Figure 6, the change in the energy absorbed by the surface had an insignificant effect on the value of the friction coefficient. Friction coefficient decrease after CPF treatment could be caused by the surface layer microhardness increase. However the surface relief also influences tribological characteristics (Kombalov, 1974; Grzesik W., 2016). The impact of the CPF causes the growth of surface roughness and waviness (Kudaktsin at. al, 2019). It should be noted that an increase in surface roughness can lead to a decrease in the coefficient of friction at the initial stage of friction. An increase in surface waviness can lead to a decrease in the actual contact area at the stage of steady-state wear and be an additional factor in reducing the friction force (Kombalov, 1974).

Conclusion

The impact of the CPF on the Cu/Ti-6Al-4V system led to the formation of a surface titanium layer alloyed by aluminum, vanadium, and copper with a uniform distribution of elements. The phase and elemental composition of the formed surface alloy, as well as its strength characteristics, depended on the energy absorbed by the surface layer.

The findings showed that plasma treatment resulted in the formation of α-Ti solid solution containing alloying elements in the surface layer and δ-TiN on the surface. Growth of the the energy absorbed by the surface led to decrease of copper concentration and increase of δ-TiN volume fraction. The increase of the energy density absorbed by the surface was also accompanied by microhardness growth leading to friction coefficient diminishing.

The work was supported by the Belarusian Republican Foundation for Fundamental Research under the grant No. T21Y-004.

References*:*

Astashinski V.M., Uglov V.V., Cherenda N.N., Shymanski V.I., Modifikaciya titana pri vozdejstvii kompressionnymi plazmennymi potokami (Modification of titanium when exposed to compressive plasma flows), Belaruskay navuka, Minsk, 2016. (In Russian).

Cherenda N.N., Basalai A.V., Uglov V.V., Laskovnev A.P., Astashynski V.M., Kuzmitski A.M. Phase composition and mechanical properties of Cu–Ti alloys synthesized in the surface layer of copper by plasma impact on the Ti/Cu system, *Vacuum*, vol. **167**, pp. 452-458, 2019.

Cherenda N.N., Laskovnev A.P., Basalai A.V., Uglov V.V., Astashynski V.M., and Kuzmitski A.M., Erosion of materials under the effect of compression plasma fows, *Inorganic Materials: Applied Research*, Vol. **6**, no. 2, pp. 114–120, 2015.

Cherenda N.N., Shimanskii V. I., Uglov V. V., Astashinskii V. M., and Ukhov V. A., Nitriding of steel and titanium surface layers under the action of compression plasma flows, *Journal of Surface Investigation. X-ray, Synchrotron and Neutron Techniques*, vol. **6**, no. 2, 319-pp. 325, 2012.

Grzesik W., Prediction of the functional performance of machined components based on surface topography: state of the art, *Journal of Materials Engineering and Performance*, vol. **25**, pp. 4460–4468, 2016.

Kaur M., Singh K., Review on titanium and titanium based alloys as biomaterials for orthopaedic applications, *Materials Science & Engineering C*, vol. **102**, pp. 844-862, 2019.

Khorasani A.M., Goldberg M., Doeven E.H., Littlefair G., Titanium in biomedical applications - properties and fabrication: a review, *Journal of Biomaterials and Tissue Engineering*, Vol. **5**, pp. 593–619, 2015.

Kombalov V.S., Vliyanie sherohovatosti tverdyh tel na trenie i iznos (Influence of Roughness of Solids on Friction and Wear), Nauka, Moscow, 1974. (In Russian).

Kudaktsin R.S., Astashynski V.M., Kuzmitski A.M., Characteristic features of the surface relief formation of metals modified by compression plasma flows, *High Temp. Mater. Process.*, vol. **23**, no. 3, pp. 275-282, 2019.

Li G., Wang Y., Qiao L., Zhao R., Zhang Sh., Zhang R., Ke Ya., Preparation and formation mechanism of copper incorporated micro-arc oxidation coatings developed on Ti-6Al-4V alloys, *Surface & Coatings Technology*, vol. **135**, pp. 74-85, 2019.

Mohammed M.T., Khan Z.A., Siddiquee A.N., Surface modifications of titanium materials for developing corrosion behavior in human body environment: a review, *Procedia Materials Science*, vol. **6**, pp. 1610–1618., 2014.

Wang X., Dong H., Liu J., Qin G., Chen D., Zhang E., In vivo antibacterial property of Ti-Cu sintered alloy implant, *Materials Science & Engineering C*, vol. **100**, pp. 38–47, 2019.

Zhang E., Li F., Wang H., Liu J., Wang Ch., Li M., Ke Ya., A new antibacterial titanium–copper sintered alloy: preparation and antibacterial property, *Materials Science & Engineering*, vol. **33** no. 7, pp. 4280-4287.

Figures caption

Fig.1. Dependence of the mass removed from surface unit area of Cu/Ti-6Al-4V system samples on the energy density absorbed by the surface.

Fig. 2. Distribution of elements Ti, Al, V and Cu along arbitrary lines on the surface of the initial sample (a) and the sample of the Cu/Ti-6Al-4V system after CPF treatment (Q= 26 J/cm^2) (b)

Fig. 3. Diffraction patterns of the Cu/Ti-6Al-4V system samples before and after CPF treatment

Fig. 4. SEM images of samples surface after CPF treatment at Q=43 J/cm^2

Fig. 5. Microhardness of Ti-6Al-4V alloy sample and Cu/Ti-6Al-4V system samples after CPF treatment at Q=26 J/cm^2 and Q=43 J/cm^2

Fig. 6. Friction coefficient dependence on the indenter sliding distance of Ti-6Al-4V sample and Cu/Ti-6Al-4V system samples after CPF treatment at Q=26 J/cm^2 and Q=43 J/cm^2

Fig.1.

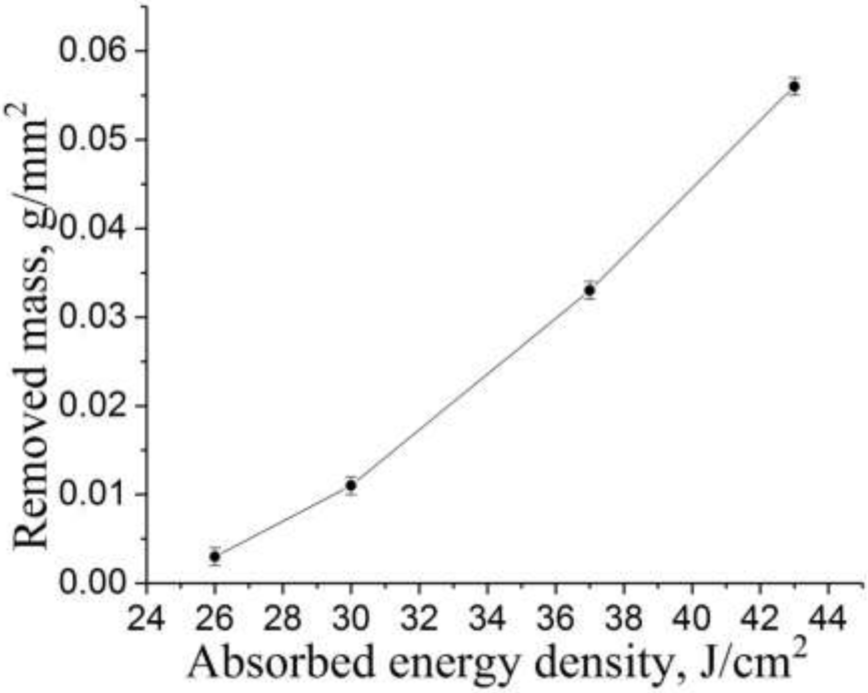
Removed mass, g/mm^2
0.00
0.01
0.02
0.03
0.04
0.05
0.06
24
26
28
30
32
34
36
38
40
42
44
Absorbed energy density, J/cm^2

Fig. 2.

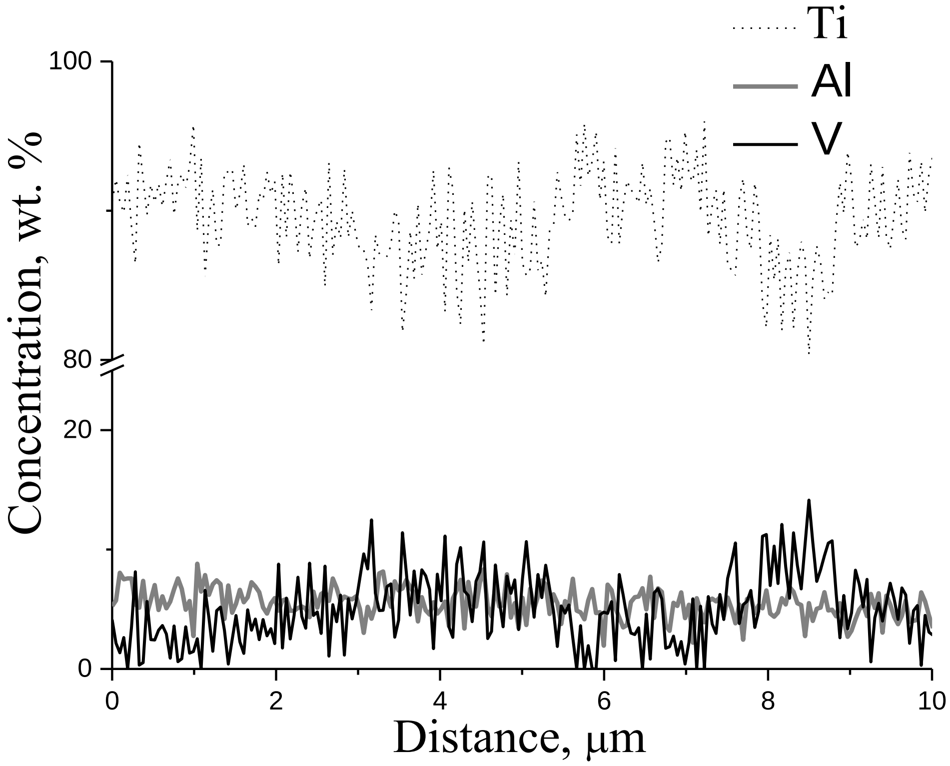
Ti
Al
V
100
80
20
0
Concentration, wt. %
0
2
4
6
8
10
Distance, μm

a

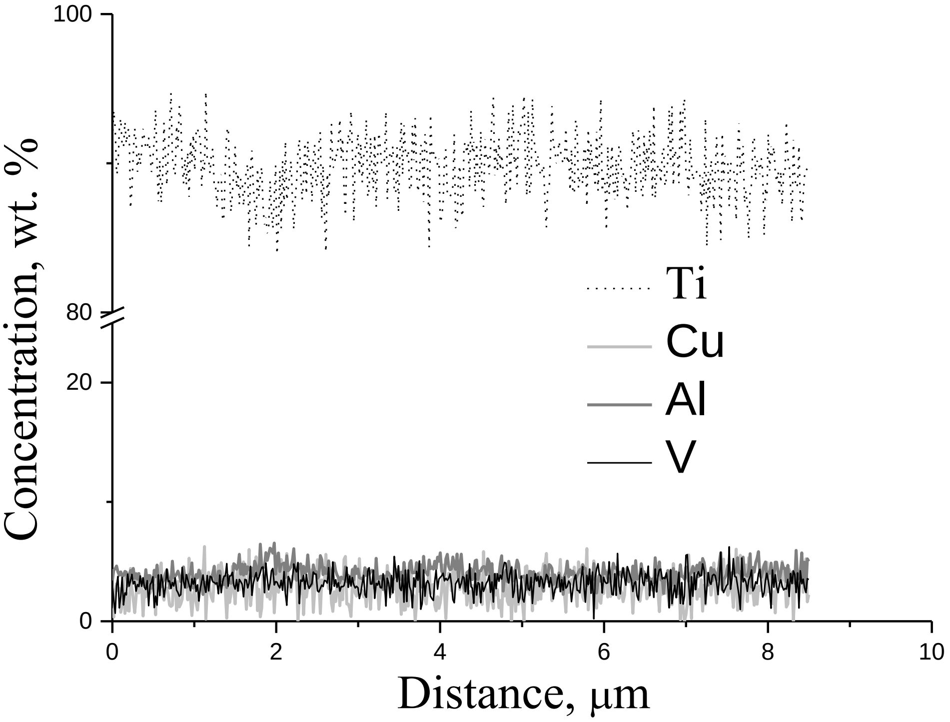
100
80
20
0
Ti
Cu
Al
V
Concentration, wt. %
0
2
4
6
8
10
Distance, μm

b

Fig. 3.

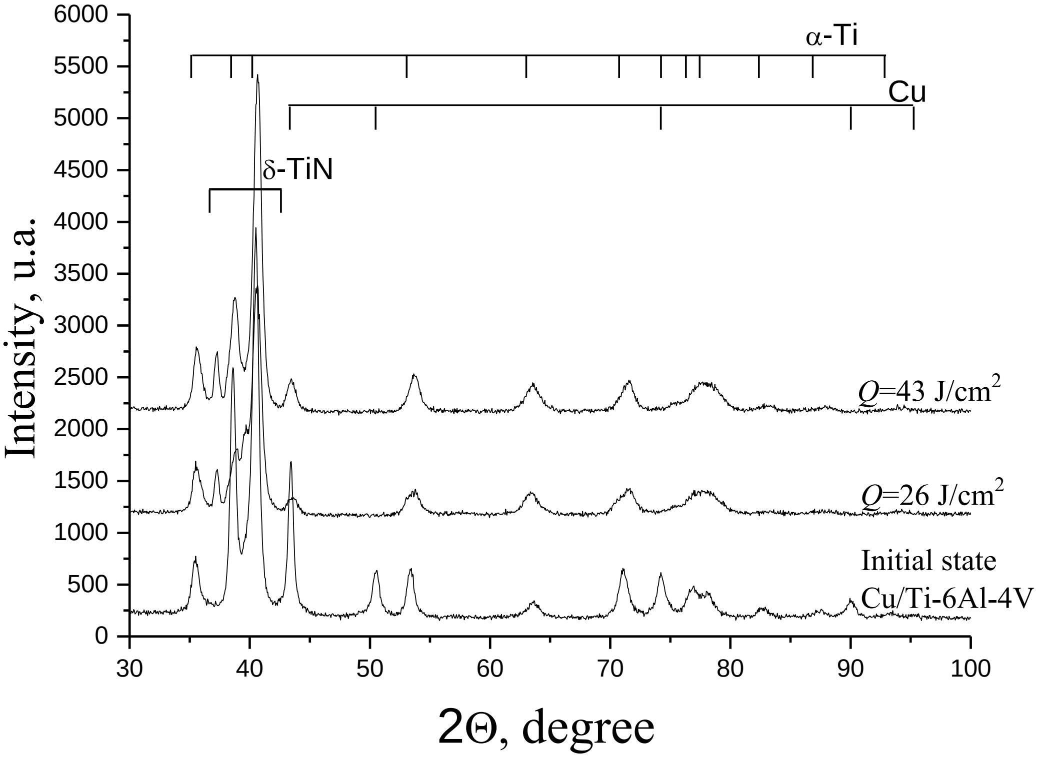
Intensity, u.a.
2Θ, degree
α-Ti
Cu
δ-TiN
Q=43 J/cm²
Q=26 J/cm²
Initial state
Cu/Ti-6Al-4V
0
500
1000
1500
2000
2500
3000
3500
4000
4500
5000
5500
6000
30
40
50
60
70
80
90
100

Fig. 4.

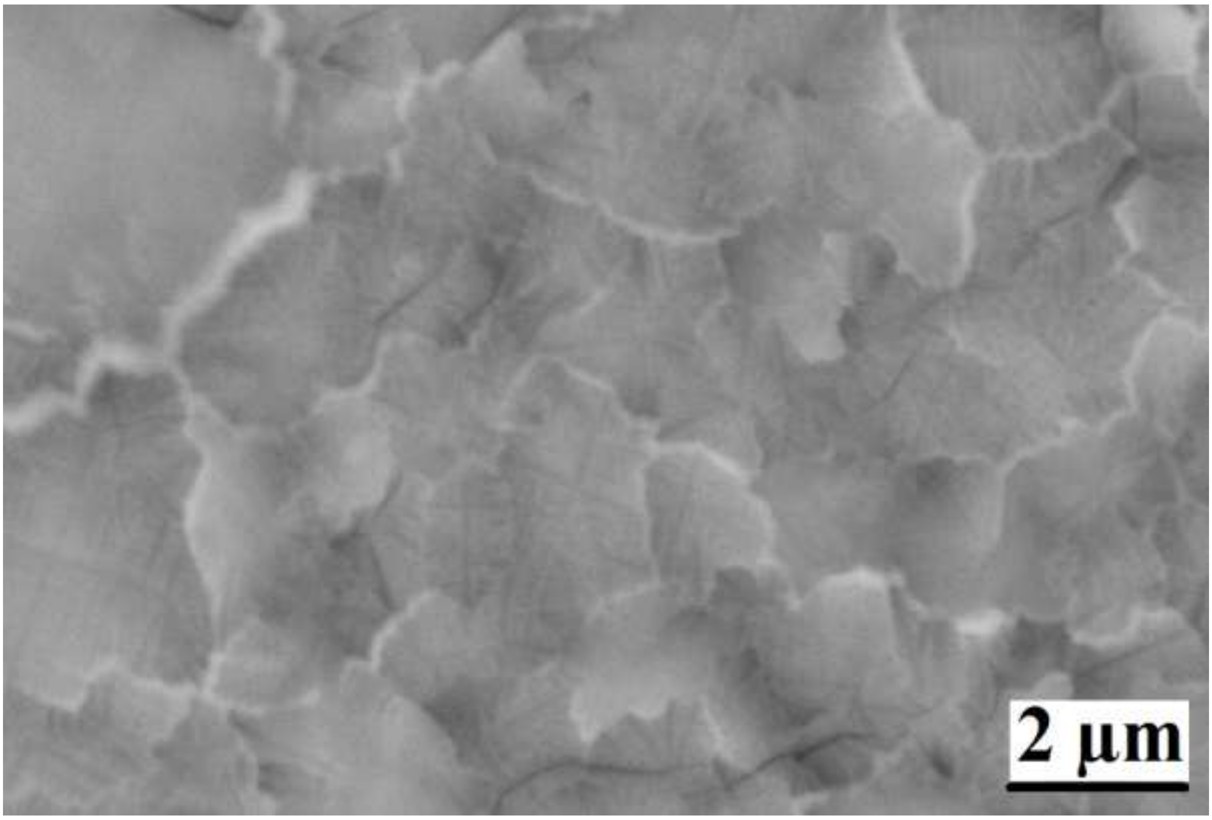

Fig. 5.

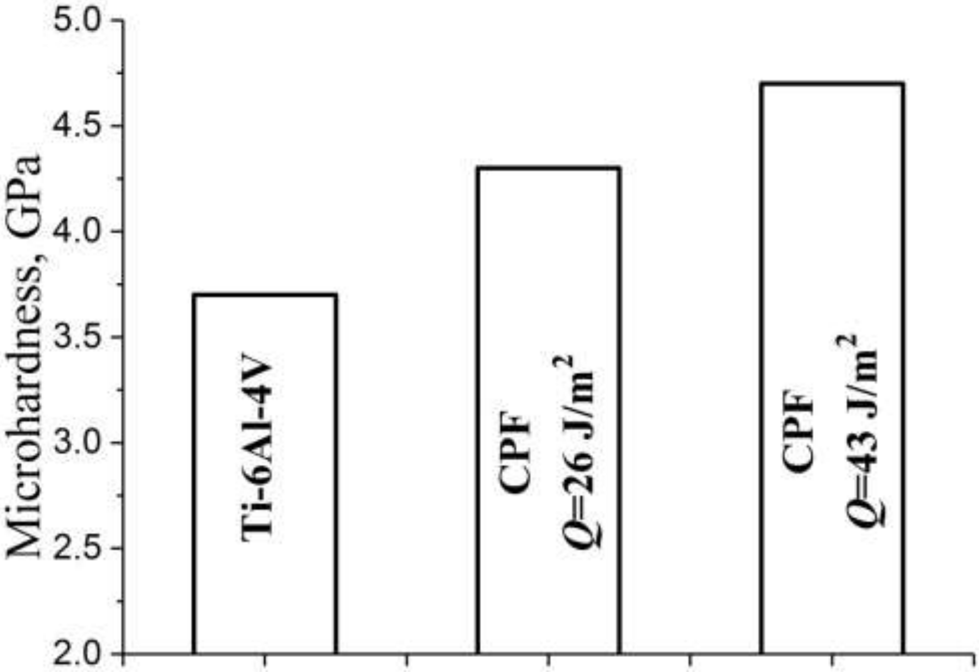
Microhardness, GPa
5.0
4.5
4.0
3.5
3.0
2.5
2.0
Ti-6Al-4V
CPF
Q=26 J/m2
CPF
Q=43 J/m2

Fig. 6.

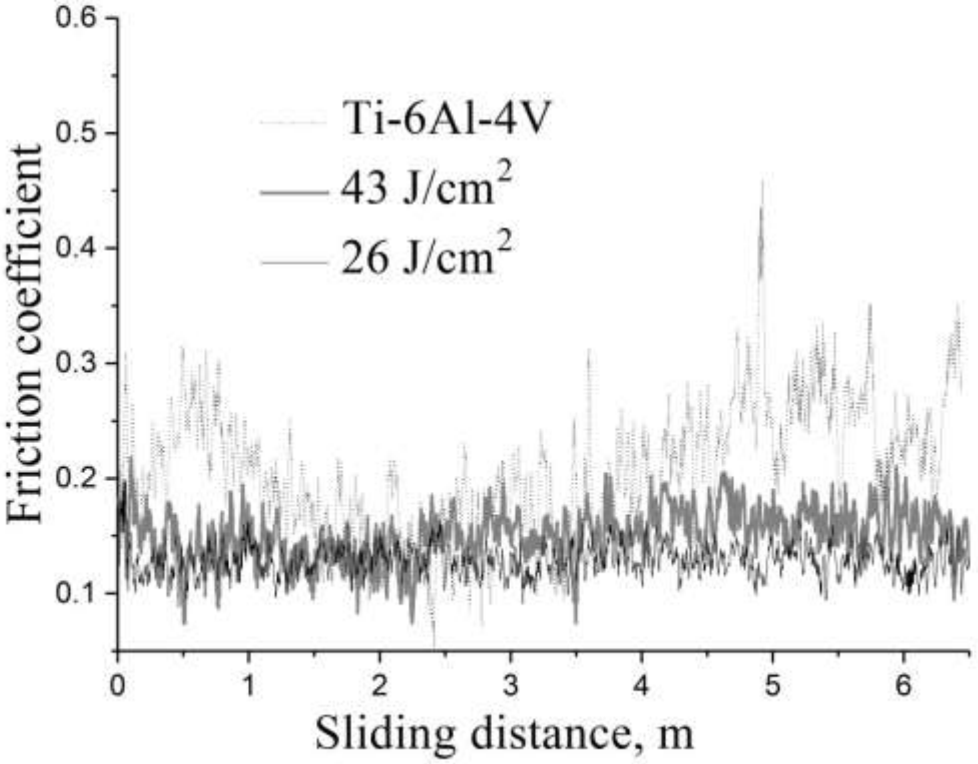
0.6
0.5
0.4
0.3
0.2
0.1
Friction coefficient
0
1
2
3
4
5
6
Sliding distance, m
Ti-6Al-4V
43 J/cm^2
26 J/cm^2